Lawrence Berkeley National Laboratory
LBL Publications

Title
Shear Resisting Mechanisms and Capacity Equations for Composite Truss Beams

Permalink
https://escholarship.org/uc/item/9t61f6ph

Journal
Journal of Structural Engineering, 141(12)

ISSN
0733-9445

Authors
Monti, Giorgio
Petrone, Floriana

Publication Date
2015-12-01

DOI
10.1061/(asce)st.1943-541x.0001266

Peer reviewed

eScholarship.org Powered by the California Digital Library
University of California

Shear Resisting Mechanisms and Capacity Equations for Composite Truss Beams

Giorgio Monti[1] and Floriana Petrone[2]

Abstract: This paper deals with the development of shear capacity equations for composite truss beams (CTBs). These equations are obtained from a purposely developed mechanics-based shear model. As opposed to commonly used approaches for the design of these structural elements, where the shear capacity is attained when the first pair of web steel bars yields, in this case the shear capacity is expressed as that causing n pairs of web steel bars to yield before concrete crushes. In this way, the performance of CTBs is maximized. Two different capacity equations are proposed: one, derived from an analytical method, explicitly takes into account the contribution of concrete to shear capacity, and the other, following most current codes, does not consider such contribution. The accuracy of the proposed capacity equations has been verified against the results of nonlinear analyses and experimental tests conceived and conducted to this aim. The comparison confirmed both the consistency of the proposed mechanical model with the experimental observations, and the capability of the capacity equations to predict the shear capacity of CTBs. **DOI: 10.1061/(ASCE)ST.1943-541X.0001266.** © *2015 American Society of Civil Engineers.*

Author keywords: Composite truss beams; Shear mechanical model; Shear capacity equations; Strain energy minimization; Experimental tests; Metal and composite structures.

Downloaded from ascelibrary.org by University of California, Berkeley on 07/19/18. Copyright ASCE. For personal use only; all rights reserved.

Introduction

Composite truss beams (CTBs) are special composite steel-concrete beams made up of precast steel trusses embedded in cast-in-place concrete. The steel truss usually consists of a web devoted to resist shear forces welded to the upper and lower chord, the latter being made of either a steel plate or a RC slab and supporting the precast floor system, as shown in Fig. 1.

The construction stage follows these steps: steel trusses are made in assembly shops, where all components are welded to each other, then they are carried to the construction site and placed between two columns by means of cranes; afterwards, slabs are placed on the lower steel-RC chord and additional rebars are mounted over the structural joints to ensure structural continuity. Once all the elements are dry-assembled, concrete is cast in place without using formworks (except for the external beams) because the steel-RC lower chord of the beams together with the slabs retains the fresh concrete. In addition, provisional propping is avoided because the steel truss is designed to sustain the construction loads.

The main advantages that led this structural system to be used in many buildings, especially if compared with ordinary steel-concrete composite structures, are the reduction of construction time and injure risk because both formworks and intermediate supports are not required, the accurate control of construction detailing performed at the workshop without in situ welding or tying, and the consequent optimization in the use of steel.

Such construction method leads to the consideration of two different structural stages characterized by two different mechanical behaviors. During the first one, beams behave as self-carrying steel structures simply supported at the ends and loaded by their self-weight, the precast floor system weight, and the weight of the fresh concrete filling. During the second stage, after concrete hardens, beams behave as special composite steel-concrete continuous beams that resist additional dead and live loads (Quaranta et al. 2010; Trentadue et al. 2011). This paper addresses the study of the shear resisting mechanisms that develop during the second stage for both cases of steel and RC lower chord.

Starting from the analysis of the well-known and fully validated shear resisting mechanisms of RC elements [e.g., Park and Paulay (1975)], a mechanical model is here developed from which a consistent closed-form shear capacity equation for CTBs is then proposed.

In spite of the widespread use of such structures for approximately 40 years, nowadays literature is quite scarce and codes do not properly address CTBs' structural behavior: the relevant equations are mainly adapted from similar composite structures or even from RC structures.

As a matter of fact, when determining the shear capacity, the variable strut angle theory traditionally used in RC does not apply because in CTBs the strut angle is known beforehand, being given by the topology of the web bars. Such theory makes use of the static limit theorem: it looks for a statically admissible (equilibrated) configuration of the resisting system made of the (fixed) steel stirrups and of the (rotating) concrete strut, both considered at their limit state (i.e., steel yielded and concrete crushed). By varying the strut angle, both the concrete and the steel contribution to the shear capacity change. The former changes because the strut contribution is projected on a different angle, the latter changes because the number of intercepted stirrups changes. When a statically admissible solution is eventually found, the static limit theorem ensures it represents a lower bound of the shear capacity (Nielsen and Braestrup 1975; Nielsen 1998; Fenwick and Paulay 1968; Connor 1976).

[1]Full Professor, Dept. of Structural and Geotechnical Engineering, Sapienza Univ. of Rome, 00197 Rome, Italy.

[2]Postdoctoral Research Associate, Dept. of Civil and Environmental Engineering, Univ. of California, Davis, CA 95616 (corresponding author). E-mail: petrone@ucdavis.edu; floriana.petrone@uniroma1.it

Note. This manuscript was submitted on February 25, 2014; approved on January 6, 2015; published online on March 17, 2015. Discussion period open until August 17, 2015; separate discussions must be submitted for individual papers. This paper is part of the ***Journal of Structural Engineering***, © ASCE, ISSN 0733-9445/04015052(11)/$25.00.

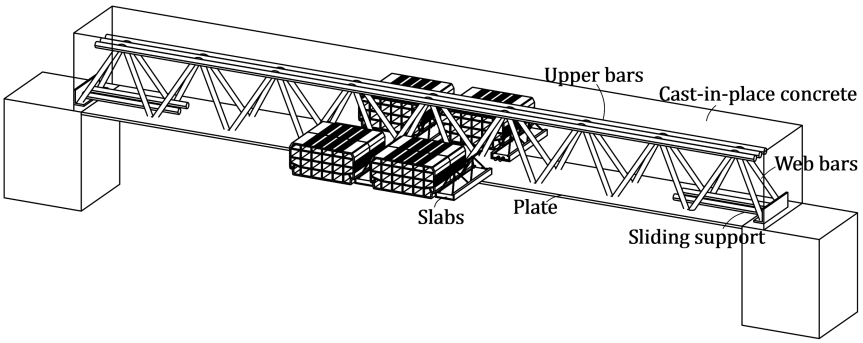

Fig. 1. CTB model

In CTBs, the shear resisting system is made of (fixed angle) web steel bars and concrete struts, whose angle depends on the truss topology; then, the shear capacity of a CTB is strictly related to its topology and its materials and cannot change as the shear demand varies, as it is for RC structures. Therefore, the shear capacity of CTBs is evaluated as follows: (1) definition of a strut-and-tie substructure representing the shear resisting model, consisting of tensile and compressive steel bars and of compressive concrete struts; (2) analysis of the statically indeterminate structure so obtained and determination of the strut size through minimization of the system strain energy; and (3) calculation of the shear capacity.

As opposed to the traditional RC shear model in which all stirrups are assumed to be yielded, the mechanical model here proposed allows following the evolution of the shear capacity as yielding progresses from the first pair of web steel bar to the subsequent ones, as long as the concrete strut does not crush.

As shown in the following sections, the capacity equations are developed on the substructure near the beam supports, where shear attains the maximum for most loading conditions. The geometry of the model is fully described through four independent parameters—width b and depth h of the beam, and spacing s and diameter ϕ of the steel bars—from which all other geometrical quantities can be derived. The considered portion of the beam is modeled as a statically indeterminate substructure made of struts and ties, the former having unknown size (Fig. 2). The system so obtained is solved through the force method, which gives the values of the forces acting in each element as function of the (unknown) struts flexibility. The solution is found by minimizing the strain energy normalized to the substructure stiffness.

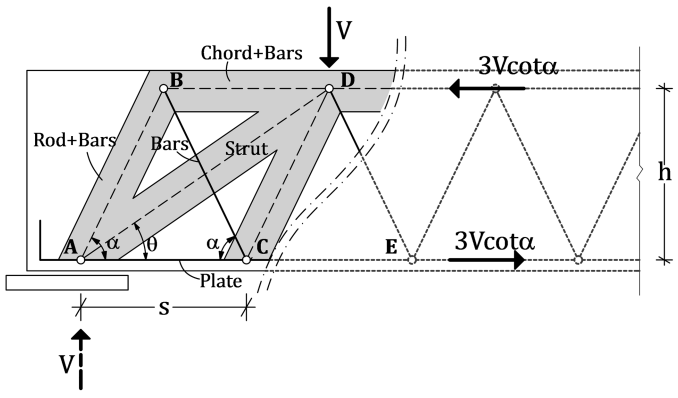

Fig. 2. Portion of a composite truss beam: notation

The application of this general procedure, hereafter called analytical method, along with the definition of shear capacity given previously, led to deriving closed-form equations to calculate the shear strength of a CTB at yielding of n pairs of tensile web steel bars. These equations allow calculating the shear capacity of a CTB by explicitly accounting for the contribution of both concrete and steel based on four parameters to describe geometry—s, ϕ, b, h—and four parameters to define materials, f_y, f_c, E_s, and E_c, that is, steel yield strength, concrete compressive strength, steel modulus, and concrete modulus, respectively.

Having developing the analytical method, a simplified (code compliant) method was derived: it is code compliant in that it does not explicitly account for the contribution of concrete to the shear capacity as required in most construction codes. It is based on four parameters, s, ϕ, f_y, h, plus the beam span L, to calculate a conservative value of the shear capacity at yielding of n pairs of web steel bars.

The accuracy of the hypotheses behind both the analytical method and the capacity equations derived from it has been checked against the results of both nonlinear analyses and experimental tests, the latter purposely conceived and performed, proving the capability of predicting the shear capacity for different typology of beams. Such comparison has been conducted also with the capacity equations resulting from the simplified method and with the so-called standard method, which is the one currently in use for CTBs design, unfortunately hampered by a significant underestimation. Detailed remarks along with some suggestions for further research are given in "Correlation Studies."

Analytical Method

The analytical method is developed under the hypothesis that both steel and concrete contribute to the shear capacity of CTBs with their strength. The capacity equations so derived explicitly account for both contributions and require the geometry of the CTB—s, ϕ, b, h—and the mechanical characteristics of materials–f_y, f_c, E_s, E_c—to be known.

In the following, the mechanical model is described in detail and its solution through the force method is shown. Then, given the new definition of shear capacity as that causing n pairs of web steel bars to yield before concrete crushes, the cases $n = 1$ and 2 are developed, yielding two different capacity equations.

Mechanical Model

In Fig. 2, a portion of a CTB near the support is shown, representing the mechanical model serving as the basis for the subsequent analytical method. The parameters describing the geometry of the

Downloaded from ascelibrary.org by University of California, Berkeley on 07/19/18. Copyright ASCE. For personal use only; all rights reserved.

model are spacing and diameter of the web steel bars, s and ϕ, respectively, and width and depth of the beam, b and h, respectively. This is clearly a statically indeterminate truss, whose members are AB and CD, inclined compressed concrete members called rods surrounding the web steel bars; BC, inclined tensile web steel bars; AD, inclined compressed concrete strut; BD, compressed upper chord made of top steel bars and concrete; and AC, bottom tensile steel plate. Members AB, BC, and CD are actually representing pairs of members, whose angle with respect to the beam vertical midplane is approximately 90°.

Because in common CTBs compressive and tensile web steel bars are equally inclined with respect to the plate, the following angles are directly obtained:

$$\alpha = \operatorname{acot}\left(0.5\frac{s}{h}\right) \quad \text{and} \quad \theta = \operatorname{acot}\left(1.5\frac{s}{h}\right) \tag{1}$$

which are the web bars angle and the inclined compression strut angle, respectively. From the two preceding equations, the following three useful relationships can be obtained as well:

$$3\cot\alpha = \cot\theta \qquad 3\sin\theta\cot\alpha = \cos\theta$$
$$2\sin\theta\cot\alpha = \cos\theta - \sin\theta\cot\alpha \tag{2}$$

which will become handy in the developments presented hereafter.

From the preceding, members' length can be readily computed

$$L_{AB} = L_{BC} = L_{CD} = \frac{s}{2\cos\alpha},$$
$$L_{AD} = \frac{3\ s}{2\cos\theta}, \qquad L_{BD} = L_{AC} = s \tag{3}$$

All members are known from both the geometric and mechanical standpoint, with the only exception the naturally formed diagonal strut AD, needed to produce a shear resisting mechanism together with the other members, whose size is still unknown.

In Table 1, the relevant geometric and mechanical properties of all members are listed. Members AB and CD are assigned the same mechanical and geometric properties.

The following positions are set:

$$\lambda_1 = \frac{L_{BC}}{L_{AD}} = \frac{1}{3}\frac{\cos\theta}{\cos\alpha} = \frac{\sin\theta}{\sin\alpha},$$
$$\lambda_2 = \frac{L_{AC}}{L_{BC}} = \frac{L_{AC}}{L_{CD}} = 2\cos\alpha, \qquad \lambda_3 = \frac{L_{AC}}{L_{AD}} = \frac{2}{3}\cos\theta \tag{4}$$

In Table 1, it can be seen that members made of concrete and steel have been homogenized into concrete through the coefficient $n_E = E_s/E_c$. Also, the strength of composite members AB, CD, and BD has been computed by assuming that when concrete crushes, the internal steel bars are already at yield.

In the following developments, the objective is that of solving the statically indeterminate structure and determining the optimal flexibility of the strut AD that minimizes the ratio of strain energy to stiffness.

Solution of the Mechanical Model

Fig. 2 shows the truss portion, simply supported at one end only, subjected to a shear force V, which is equilibrated by two horizontal forces, equal to $3V\cot\alpha$, corresponding to the moment applied by the remaining portion of the beam.

The statically indeterminate truss can be conveniently solved through the force method, where two statically determined systems are used: one, denoted as primary–statically determinate (ISO), obtained by removing the strut AD, and the other, denoted as redundant (RED), where the corresponding unknown redundant internal force is applied to the system ISO. After solving the two systems, the compatibility equation is written as follows:

$$n_{AD}(f_{AD}) = \frac{V}{\sin\theta}\frac{\Delta^{ISO}}{\Delta^{RED}(f_{AD})} \tag{5}$$

where Δ^{ISO} = flexibility coefficient relevant to the relative displacement of nodes A and D in the system ISO; and Δ^{RED} = flexibility coefficient relevant to the relative displacement of nodes A and D in the system RED, given, respectively, by

$$\Delta^{ISO} = \lambda_1^2(f_{BC} + 2f_{CD}) + \frac{1}{2}\lambda_3^2(2f_{BD} - f_{AC}) \tag{6}$$

$$\Delta^{RED}(f_{AD}) = \lambda_1^2(f_{BC} + 2f_{CD}) + \lambda_3^2(f_{BD} + f_{AC}) + f_{AD} \tag{7}$$

where $f_i = L_i/E_iA_i$ is the flexibility of member i. Therefore, Eqs. (6) and (7) can be easily derived by making use of the expressions in Eq. (4) that require the geometry of the truss to be known.

It is expedient to define the quantity

$$\bar{X} = \lambda_1^2(f_{BC} + 2f_{CD}) + \lambda_3^2(f_{BD} + f_{AC}) \tag{8}$$

so to obtain

$$\Delta^{ISO} = \bar{X} - \frac{3}{2}\lambda_3^2 f_{AC} \tag{9}$$

$$\Delta^{RED}(f_{AD}) = \bar{X} + f_{AD} \tag{10}$$

Notice that

$$\Delta^{RED}(f_{AD}) - \Delta^{ISO} = f_{AD} + \frac{3}{2}\lambda_3^2 f_{AC} \tag{11}$$

Also notice that the derivatives with respect to f_{AD} are

$$\frac{\partial\Delta^{ISO}}{\partial f_{AD}} = 0, \qquad \frac{\partial\Delta^{RED}(f_{AD})}{\partial f_{AD}} = 1 \tag{12}$$

Once the unknown force in member AD is found [Eq. (5)], which is in turn a function of its still unknown flexibility, all other member forces can be computed from equilibrium (Fig. 2) as

Table 1. Geometric and Mechanical Properties of All Members

Member	AB, CD (rod + bars)	BC (bars)	AD (strut)	BD (chord + bars)	AC (plate)
Angle	α	α	θ	0	0
Length	$s/2\cos\alpha$	$s/2\cos\alpha$	$3s/2\cos\alpha$	s	s
Elastic model	E_c	E_s	E_c	E_c	E_s
Strength	$f_cA_{rod} + f_yA_b$	f_y	f_c	$f_cA_{cho} + f_yA_{top}$	f_y
Area	$A_{rod} + n_EA_b$	A_b	A_{strut}	$A_{cor} + n_EA_{top}$	A_p

Downloaded from ascelibrary.org by University of California, Berkeley on 07/19/18. Copyright ASCE. For personal use only; all rights reserved.

$$n_{AB}(f_{AD}) = n_{BC}(f_{AD}) = n_{CD}(f_{AD}) = \frac{V}{\sin\alpha}\left[1 - \frac{\Delta^{ISO}}{\Delta^{RED}(f_{AD})}\right] \tag{13}$$

$$n_{BD}(f_{AD}) = 2V\cot\alpha\left[1 - \frac{\Delta^{ISO}}{\Delta^{RED}(f_{AD})}\right] \tag{14}$$

$$n_{AC}(f_{AD}) = V\left\{\left[1 - \frac{\Delta^{ISO}}{\Delta^{RED}(f_{AD})}\right]\cot\alpha + \frac{\Delta^{ISO}}{\Delta^{RED}(f_{AD})}\cot\theta\right\} \tag{15}$$

At this stage of the mechanical model's solution, all quantities are expressed as a function of the unknown flexibility of the member AD, f_{AD}.

Yielding of the First Tensile Bars: $n = 1$

When $n = 1$, the shear capacity is defined as the shear value causing the tensile bar BC [Fig. 2 and Eq. (13)] to yield, which is found by imposing

$$n_{BC}(f_{AD}) = \frac{V_y}{\sin\alpha}\left(1 - \frac{\Delta^{ISO}}{\Delta^{RED} f_{AD}}\right) = f_y A_b = n_{BC} \tag{16}$$

From which, the shear capacity is found as

$$V_{y1}(f_{AD}) = f_y A_b \sin\alpha\left[1 - \frac{\Delta^{ISO}}{\Delta^{RED}(f_{AD})}\right]^{-1} = f_y A_b \sin\alpha\left[\frac{\Delta^{RED}}{\Delta^{RED}(f_{AD}) - \Delta^{ISO}}\right] \tag{17}$$

The shear capacity is still unknown because it depends on the unknown value of the flexibility of the member AD.

Moreover, when the tensile bar BC yields, the forces in all members are directly determined by replacing $V_{y1}(f_{AD})$ in the corresponding equations. Recalling the relationships in Eq. (2), the forces are then

$$n_{AB} = n_{CD} = f_y A_b \tag{18}$$

$$n_{BD} = 2 f_y A_b \cos\alpha = \lambda_2 f_y A_b \tag{19}$$

$$n_{AD}(f_{AD}) = f_y A_b \frac{\sin\alpha}{\sin\theta}\frac{\Delta^{ISO}}{\Delta^{RED}(f_{AD}) - \Delta^{ISO}} = f_y A_b \frac{1}{\lambda_1}\frac{\Delta^{ISO}}{\Delta^{RED}(f_{AD}) - \Delta^{ISO}} \tag{20}$$

$$n_{AC}(f_{AD}) = f_y A_b \sin\alpha\left[1 - \frac{\Delta^{ISO}}{\Delta^{RED}(f_{AD})}\right]^{-1} \times \left\{\left[1 - \frac{\Delta^{ISO}}{\Delta^{RED}(f_{AD})}\right]\cot\alpha + \frac{\Delta^{ISO}}{\Delta^{RED}(f_{AD})}\cot\theta\right\} = f_y A_b \frac{\lambda_2}{2}\left[1 + 3\frac{\Delta^{ISO}}{\Delta^{RED}(f_{AD}) - \Delta^{ISO}}\right] \tag{21}$$

Minimization of Strain Energy

The value of the flexibility can be found by minimizing, with respect to f_{AD}, the following function, representing the strain energy normalized to the stiffness:

$$\varepsilon(f_{AD}) = \sum_i \frac{n_i(n_i f_i)}{k_i} = \sum_i n_i^2 f_i^2 \tag{22}$$

where n_i and f_i = axial force and, again, the stiffness in member i.

For the case at hand, Eq. (22) becomes

$$\varepsilon(f_{AD}) = n_{AB}^2 f_{AB}^2 + n_{CD}^2 f_{CD}^2 + n_{AD}^2(f_{AD}) f_{AD}^2 + n_{AC}^2(f_{AD}) f_{AC}^2 + n_{BD}^2 f_{BD}^2 + n_{BC}^2 f_{BC}^2 \tag{23}$$

Given that the flexibilities and the axial forces of AB and CD are equal, Eq. (22) can be written as

$$\varepsilon(f_{AD}) = 2n_{CD}^2 f_{CD}^2 + n_{AD}^2(f_{AD}) f_{AD}^2 + n_{AC}^2(f_{AD}) f_{AC}^2 + n_{BD}^2 f_{BD}^2 + n_{BC}^2 f_{BC}^2 \tag{24}$$

Only the axial forces in AD and AC are functions of the flexibility f_{AD} [Eqs. (20) and (21)]. The derivatives of these axial forces are

$$\frac{\partial n_{AD}(f_{AD})}{\partial f_{AD}} = -f_y A_b \frac{1}{\lambda_1}\frac{\Delta^{ISO}}{[\Delta^{RED}(f_{AD}) - \Delta^{ISO}]^2} \tag{25}$$

$$\frac{\partial n_{AC}(f_{AD})}{\partial f_{AD}} = -f_y A_b \frac{3}{2}\lambda_2 \frac{\Delta^{ISO}}{[\Delta^{RED}(f_{AD}) - \Delta^{ISO}]^2} \tag{26}$$

Then minimization of the strain energy with respect to f_{AD} is carried out

$$\frac{\partial \varepsilon(f_{AD})}{\partial f_{AD}} = 2n_{AD}(f_{AD})\frac{\partial n_{AD}(f_{AD})}{\partial f_{AD}} f_{AD}^2 + 2n_{AD}^2(f_{AD}) f_{AD} + 2n_{AC}(f_{AD})\frac{\partial n_{AC}(f_{AD})}{\partial f_{AD}} f_{AC}^2 = 0 \tag{27}$$

By replacing the corresponding derivatives and axial forces [Eqs. (25) and (26)], one has

$$\frac{\Delta^{ISO}}{\Delta^{RED}(f_{AD}) - \Delta^{ISO}}(f_y A_b)^2 \times \left\{-\frac{1}{\lambda_1^2}\frac{\Delta^{ISO}}{[\Delta^{RED}(f_{AD}) - \Delta^{ISO}]^2} f_{AD}^2 + \frac{1}{\lambda_1^2}\frac{\Delta^{ISO}}{\Delta^{RED}(f_{AD}) - \Delta^{ISO}} f_{AD} - \frac{3}{4}\lambda_2^2\left[1 + 3\frac{\Delta^{ISO}}{\Delta^{RED}(f_{AD}) - \Delta^{ISO}}\right]\frac{1}{\Delta^{RED}(f_{AD}) - \Delta^{ISO}} f_{AC}^2\right\} = 0 \tag{28}$$

After some algebraic manipulations and solving for f_{AD}, one obtains

$$f_{AD} = \frac{\frac{2}{3} f_{AC}^2 \cos^2\theta + 3\Delta^{ISO} f_{AC}}{2\Delta^{ISO} - f_{AC}} \tag{29}$$

Once the flexibility of the strut is found, its area is

$$A_{strut} = A_{AD} = \frac{L_{AD}}{E_c f_{AD}} \tag{30}$$

Therefore, the shear capacity at yielding of the first pair of tensile web bars is then found by replacing the value just found into

Downloaded from ascelibrary.org by University of California, Berkeley on 07/19/18. Copyright ASCE. For personal use only; all rights reserved.

$$V_{y1}(f_{AD}) = f_y A_b \sin\alpha \left(\frac{f_{AD} + \bar{X}}{f_{AD} + \frac{2}{3} f_{AC} \cos^2\theta} \right) \tag{31}$$

The term in parentheses represents the increase in shear capacity due to the strut with respect to considering only the contribution of the web steel bars, given by $f_y A_b \sin\alpha$. This contribution is exactly the one that the strut offers at the time the first pair of tensile web bars yields.

Yielding of the Second Tensile Bars: n = 2

When determining the shear capacity for the case $n = 2$, that is, the shear value causing member DE to yield, the contribution of the strut changes. Starting from the results obtained from the preceding procedure, the shear capacity V_{y2} can be calculated as

$$V_{y2}(f_{AD}) = f_y A_b \sin\alpha \left[\frac{\Delta^{ISO}}{\Delta^{RED}(f_{AD}) - \Delta^{ISO}} \left(1 - \frac{2s}{L} \right)^{-1} + 1 \right] \tag{32}$$

where L = CTB span.

The V_{y2} can be actually attained if the cross-sectional area of the strut at yielding of the second pair of bars meets the following condition:

$$A_{strut.2} \le A_{max} \tag{33}$$

where $A_{strut.2} = A_{strut} \cdot (1–2s/L)^{-1}$; and $A_{max} = b \cdot s$.

Nonlinear analyses, shown hereafter, proved that the condition in Eq. (33) is fulfilled for the most common CTB topologies.

The capacity equations here proposed derive from the simplest shear mechanical model of CTBs that can actually apply in the most common topologies of CTBs.

After all, the procedure explained previously can be conveniently used to obtain shear capacity equations for any topology of CTBs, where any other shear resisting mechanism is proved to be active.

Simplified (Code Compliant) Method

A simplified method has been derived from the analytical one, explained in the previous section. Though stemming from the same interpretation of the mechanical behavior of CTB, it is developed under the consideration that concrete contributes to the increase in shear capacity with its stiffness, rather than with its strength. This implies that the concrete strut is capable of sustaining the force increase consequent to yielding of the first web steel bars until the subsequent web steel bars yield as well (Fig. 3). The capacity equation so derived depends on s, ϕ, f_y, h, and L.

The aim is that of obtaining an accurate capacity equation suitable for practical use, which fulfils the basic requirement of most construction codes of neglecting the contribution of the concrete strength to the shear capacity.

The shear capacity is then expressed as

$$V = \kappa f_{yd} A_b \sin\alpha \tag{34}$$

with

$$\kappa = \frac{n_t - 2(1 - \delta_p)}{n_t - 2(n_s - \delta_p)} \tag{35}$$

where n_t = overall number of tensile web steel bars of the CTB easily calculated from s and L; $n_s = n$ is the number of tensile web steel bars that yield; and from elementary statics

$$\delta_p = \begin{cases} 0 & \text{load applied at the top of the beam} \\ 1 & \text{load applied at the bottom of the beam} \end{cases}$$

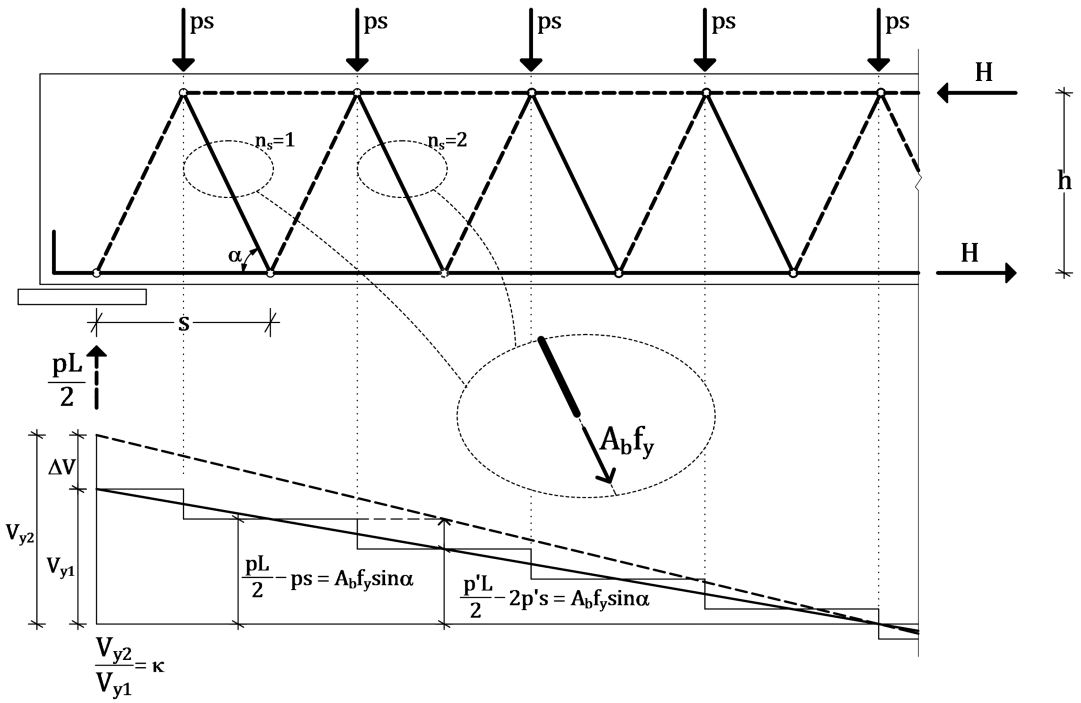

Fig. 3. Simplified model: graphic representation of κ; between yield of the first and second steel bar, the shear diagram shifts upwards, thus producing the increase ΔV

Downloaded from ascelibrary.org by University of California, Berkeley on 07/19/18. Copyright ASCE. For personal use only; all rights reserved.

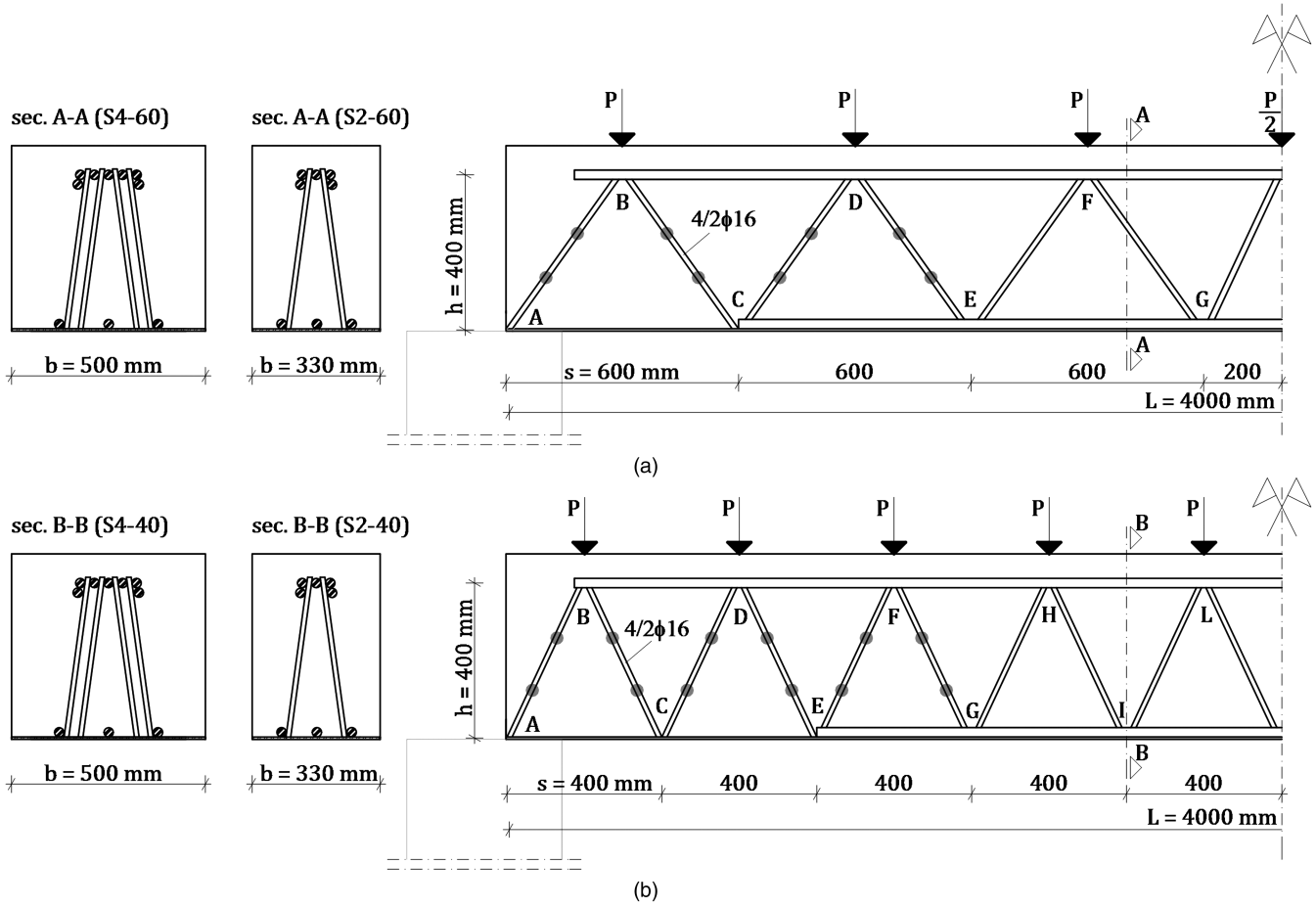

Fig. 4. Models for nonlinear analyses: (a) sample S4-60/S2-60; (b) sample S4-40/S2-40

Nonlinear Analyses

For the purpose of validating the proposed mechanical model and the capacity equations derived from it, the preceding equations have been tested against nonlinear analyses.

The nonlinear analyses have been developed with the open-source platform *OpenSees* in which each truss element was assigned nonlinear properties at the material level: steel was modeled using a uniaxial bilinear law (Steel01 Material), whose main properties were specified on the basis of 20 experimental tensile tests conducted on this purpose (see the Appendix). The concrete constitutive model for the shear resisting elements explicitly accounts for the stiffness increase of the inclined concrete strut consequent to the yielding of the steel bars. Such a phenomenon follows the analytical description obtained in Eqs. (30) and (33). As for the upper chord concrete, a uniaxial Kent and Park (1971) [modified by Scott et al. (1982)] constitutive law (Concrete01 Material, zero tensile strength) is used, where the ultimate strength of concrete in the Appendix derives from 24 compressive experimental tests on concrete cubes.

The study has been conducted on different types of CTB by varying some of the geometrical parameters describing its topology.

The results shown in the following refer to the geometric and mechanical properties of four of the eight full-scale samples tested in the experimental campaign that will be presented in the next section (Fig. 4 and Table 2).

Table 2. Specimens: Geometry and Reinforcement

Specimen identifier	$b \times h$ (mm)	Span (mm)	Reinforcement		
			Shear	Top	Bottom (mm)
S2-60	330×400	4,000	$2\phi16$	$5\phi30$	Steel plate $300 \times 8(L = 4{,}000) + 3\phi30(L = 2{,}800)$
S2-40					Steel plate $330 \times 8(L = 4{,}000) + 3\phi30(L = 2{,}400)$
C2-60					$4\phi30\ (L = 4{,}000) + 2\phi30(L = 2{,}800)$
C2-40					$4\phi30\ (L = 4{,}000) + 2\phi30(L = 2{,}400)$
C4-60	500×400		$4\phi16$	$7\phi32$	$6\phi32\ (L = 4{,}000) + 2\phi32(L = 2{,}800)$
C4-40					$6\phi32\ (L = 4{,}000) + 2\phi32(L = 2{,}400)$
S4-60					Steel plate $500 \times 10(L = 4{,}000) + 3\phi32(L = 2{,}800)$
S4-40					Steel plate $500 \times 10(L = 4{,}000) + 3\phi32(L = 2{,}400)$

Note: The bottom reinforcement is usually made of a steel plate with reinforcing steel bars welded along it at midspan.

Downloaded from ascelibrary.org by University of California, Berkeley on 07/19/18. Copyright ASCE. For personal use only; all rights reserved.

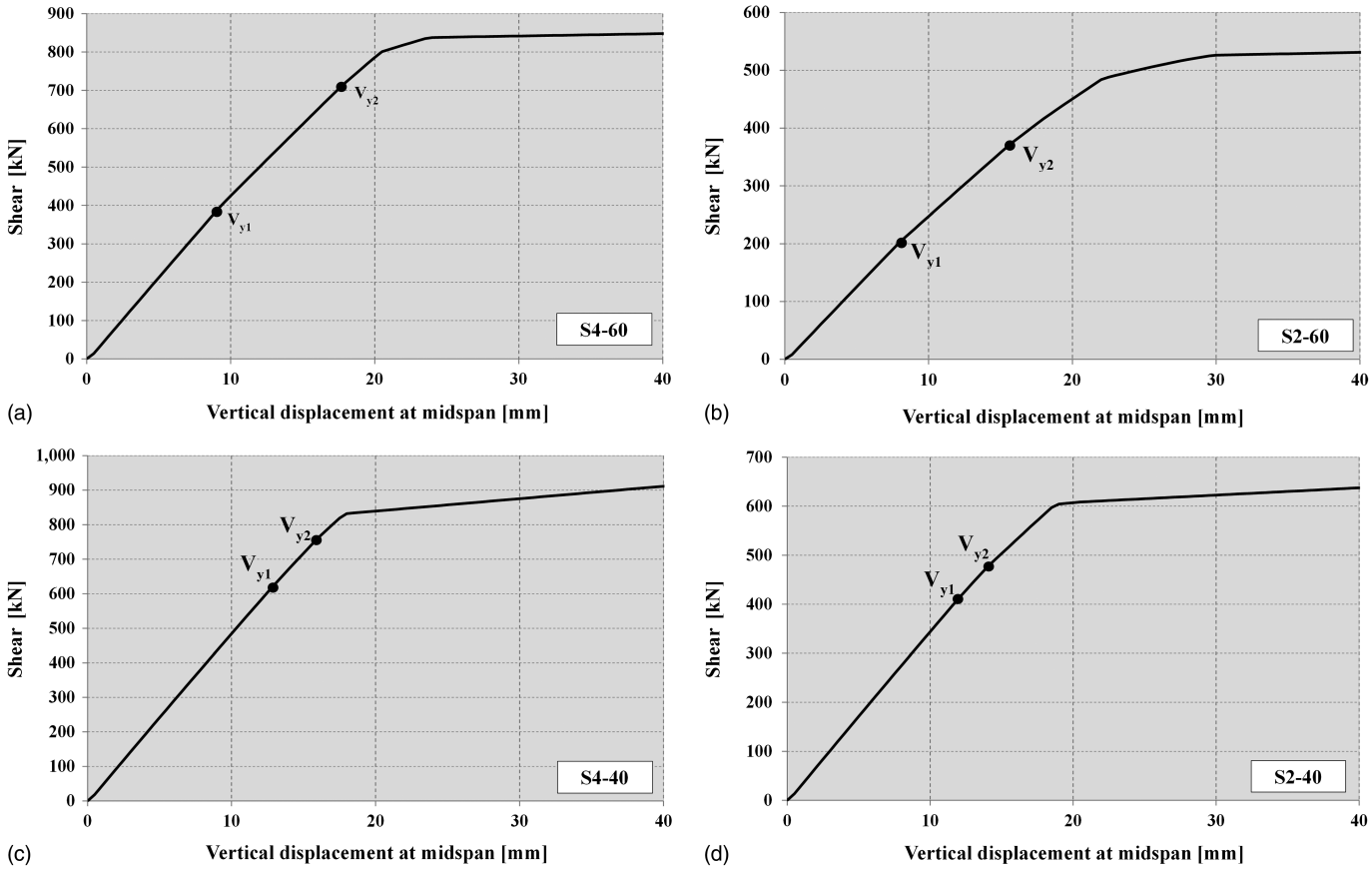

Fig. 5. Shear displacement law: V_{y1} and V_{y2} for (a) S4-60; (b) S2-60; (c) S4-40; (d) S2-40

A displacement-controlled analysis has been performed on simply supported beams representing the specimens in order to analyze the failure sequence of the resisting elements and to check the corresponding resisting shear value. The strain-based failure criterion is implicitly assigned with the constitutive laws for both steel and concrete.

Fig. 5 shows the shear–midspan vertical displacement curves of beams S4-60, S2-60, S4-40, and S2-40: the values of the shear capacity V_{y1}, at yielding of the first web steel bar, and V_{y2}, at yielding of the second web steel bar, are highlighted along the curve, showing that for all the cases the failure sequence is the same hypothesized in the proposed mechanical model.

Fig. 6. Experimental setup: sample: (a) S4-60; (b) C2-60

Downloaded from ascelibrary.org by University of California, Berkeley on 07/19/18. Copyright ASCE. For personal use only; all rights reserved.

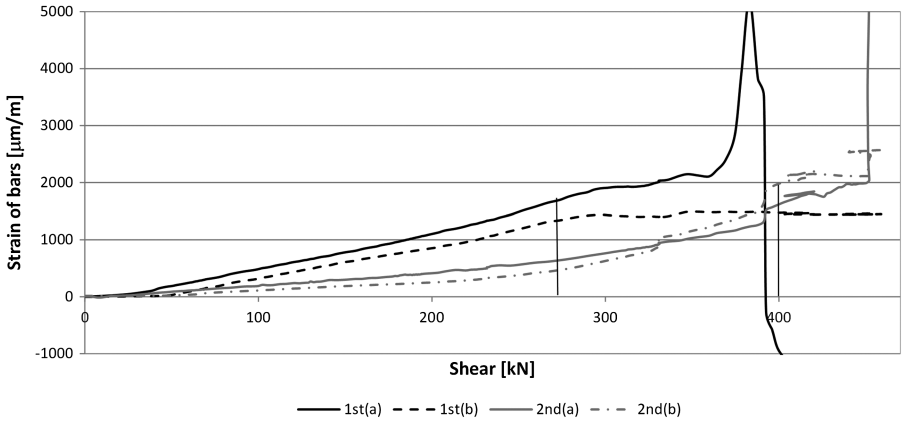

Fig. 7. Sample S2-60: shear strain of bars

All the curves are characterized by a quasi-linear branch up to a flat peak that marks the flexure failure of the beam, which is actually an expected behavior because all the beams have been designed according to capacity design criteria. Moreover, the graphs show a quite large increase of shear after the yielding of the second tensile bar and before the flexure crisis occurs, meaning that there still is a reserve of capacity that ensures prevention of sudden failures. Most importantly, it is noticed that the gain in shear capacity, from V_{y1} to V_{y2}, is quite significant.

From the results of nonlinear analyses it has also been possible to verify the failure sequence of CTB resisting elements: the analyzed beams reach their ultimate state for flexural failure after the yielding of two couples of tensile bars and when the concrete strut is not yet crushed, so confirming the pseudoductile shear behavior from which the proposed equations are derived.

Experimental Tests

Eight full-scale beams have been designed and tested to verify the mechanical model and the equations here proposed. Table 2 summarizes the geometric characteristics and the reinforcement details of the specimens and the Appendix reports the materials properties. Specimen identifiers have the following meaning: the first letter refers to the material of the lower chord—S denotes steel, C denotes RC—the second letter refers to the number of web steel

Fig. 8. Samples (a and b) C2-60; (c and d) S2-60

Downloaded from ascelibrary.org by University of California, Berkeley on 07/19/18. Copyright ASCE. For personal use only; all rights reserved.

Table 3. Comparison of Results

Sample	Shear (kN)	Experimental results		Nonlinear analyses	Analytical method	Simplified method	Standard method
		Concrete	Steel				
2-60	V_{y1}	230	270	203	251	—	125
	V_{y2}	290	400	368	336	209	—
	V_C	—	—	484[a]	492	—	—
2-40	V_{y1}	442	516	412	338	—	138
	V_{y2}	514	571	476	404	184	—
	V_C	—	—	597[a]	618	—	—
4-60	V_{y1}	600	500	385	489	—	251
	V_{y2}	712	—	704	649	418	—
	V_C	—	—	801[a]	936	—	—
4-40	V_{y1}	743	751	627	654	—	276
	V_{y2}	874	879	761	780	368	—
	V_C	—	—	819[a]	1,176	—	—

[a]Yielding of lower chord.

bars in the cross section—either 2 or 4—and the number after the dash refers to the bar spacing, expressed in centimeters.

As opposed to what is usually done in shear tests, the authors decided to test the CTBs under a distributed load [Figs. 4 and 6(a and b)] instead of performing the usual three-point bending test. The authors are in fact convinced that only in this way can the entire truss be activated, rather than when a single jack applies the load, which is directly transferred by the truss towards the support. For simulating a distributed load along the beam, forces have been applied on each top node of the truss by means of hydraulic jacks coupled with a loading control unit. Applying a distributed loading also required a continuous and accurate monitoring of the pressure of the jacks in order to maintain the force equal on each node when the structure is deflected. During the tests, each beam has been monitored with couples of strain gauges placed on each diagonal steel bar of the supporting zone (gray spots in Fig. 4) and with one linear variable displacement transducer (LVTD) placed at mid-span. No strain gauges were placed along the top and bottom chords because they were designed to remain into the elastic range.

Fig. 7 shows how the strain of the tensile bars changes under increasing shear: in detail, the curves denoted with 1st (a) and (b) refer to the couple of strain gauges on the first tensile bar (BC in Fig. 2) and the curves denoted with 2nd (a) and (b) (DE in Fig. 2) to the strain gauges of the second tensile bar. The first couple of tensile bars, BC, yields before the second one, DE, when shear forces attain 270 and 400 kN, respectively, because the curves labeled with 1st (a) and (b) become flat before the curves labeled with 2nd (a) and (b). Although the two lines labeled 1st (a) and (b) are not overlapped as well as the two lines labeled 2nd (a) and (b), which is due to the imprecisions affecting any experimental measurements, the tests confirm the failure sequence of the shear resisting elements. Also, the peak attained by the solid line labeled 1st (a) and the solid line labeled as 2nd (a) is clearly due to a breakage of the strain gauge.

Moreover, Fig. 8, showing the crack pattern of beams C2-60 and S2-60 after increasing the load beyond flexural failure, demonstrates that the concrete strut actually forms, thus confirming that the mechanical model here proposed fully complies with the observed experimental behavior.

Correlation Studies

In this section, the capability of the proposed mechanical model of predicting the real structural behavior is verified and, at the same time, the accuracy of the capacity equations derived from it is assessed. On this purpose, the results obtained from nonlinear analyses and experimental tests have been compared with those of both the analytical and the simplified model. Comparisons have been also made with the so-called standard method (Superior Council of Public Works Guidelines 2009), the one currently used to design CTBs in shear, which roughly considers the shear capacity equal to the shear causing the first tensile web steel bar to yield. That is, referring to Eq. (34), $V_{\mathrm{Rdn}} = \kappa f_{yd} A_{bn} \sin\alpha$, with $\kappa = 1$.

Table 3 lists the values of V_{y1}, V_{y2}, and V_C, the latter being the theoretical shear capacity at concrete strut crushing, of all the samples obtained from experiments, nonlinear analyses, proposed

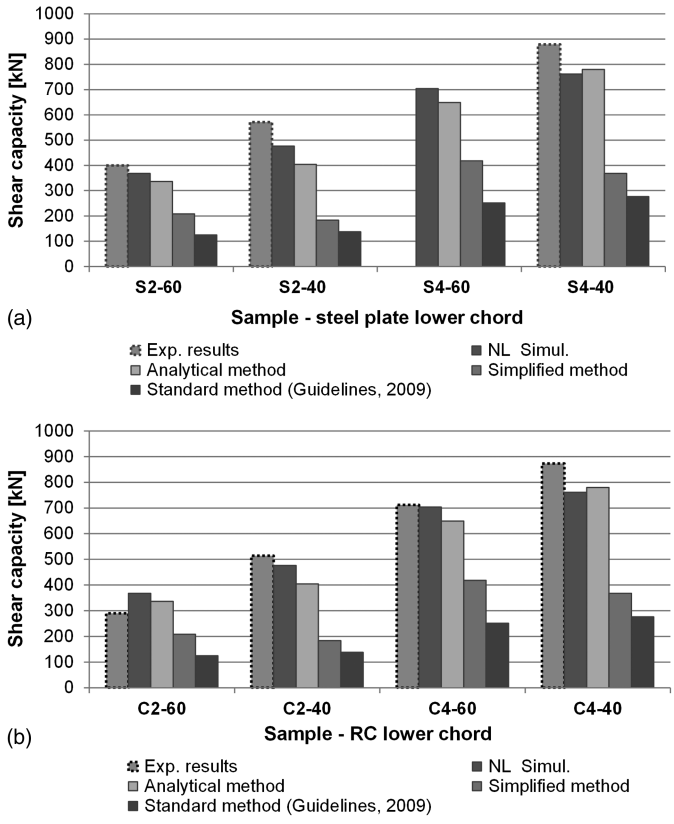

Fig. 9. Comparison among different methods for predicting the experimental shear capacity of CTBs with (a) steel plate lower chord; (b) RC lower chord

Downloaded from ascelibrary.org by University of California, Berkeley on 07/19/18. Copyright ASCE. For personal use only; all rights reserved.

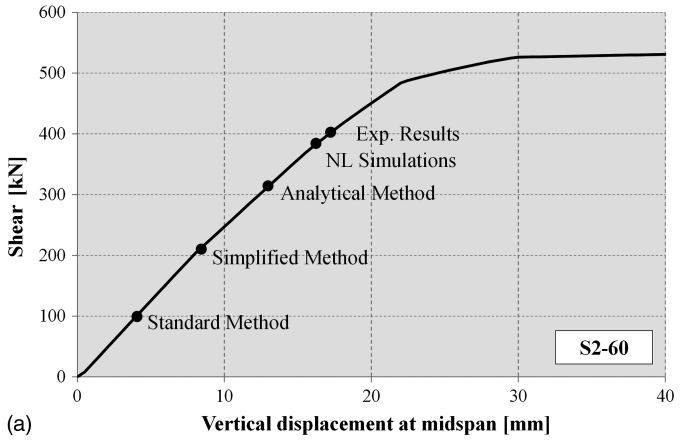

Fig. 10. Samples (a) S2-60; (b) S2-40 shear displacement curve

methods—analytical and simplified (code compliant)—and the standard method. The same data are plotted in Figs. 9(a and b) as well. Starting from these results, some remarks useful for evaluating the accuracy of each model and formulation can be highlighted: the comparison between experiments and nonlinear analyses proves how much the model adopted for numerical simulations is able to represent the real behavior of CTBs observed during the experimental tests. This way, the model can be easily adapted to simulate the behavior of any beam configuration. As shown in Table 3, the error in the estimate of the shear capacity at yielding of the second couple of steel bars varies from 1 to 15%, which is deemed to be a good agreement. Then the comparison between experimental results and the analytical method aims at showing the accuracy of the proposed capacity equations: the difference in the obtained values, which is 14% on the average, should be regarded as an acceptable approximation in any analytical model. In fact, the overall shear resistance of a composite member depends on several primary and secondary resisting mechanisms: experimental tests and nonlinear analyses account for all these mechanisms by nature, while mechanics-based analytical models do not, trying to capture and reproduce the main resisting mechanism that governs the shear behavior. For this reason, the results of this comparison are considered satisfactory. However, the proposed analytical method, along with the capacity equations derived from it, can be certainly improved in future studies by including more resisting mechanisms that are proved to be active in CTBs.

Moreover, as expected, the simplified (code compliant) method, which allows for calculating the shear capacity without explicitly considering the contribution of concrete by using very simple formulations, gives a lower and more conservative estimate of the shear capacity with respect to the analytical model. When comparing the results of the simplified (code compliant) method with the standard one currently in use, the difference in the shear capacity become significantly high, demonstrating that even the simplified (code compliant) method allows for an optimization of the shear design.

In Fig. 10 the values of the shear capacity V_{y2} obtained from all the analyses for the sample S2-60 and from the sample S2-40 are highlighted along the shear-midspan displacement curve: these graphs show that both the simplified and the analytical model give a conservative value of the shear capacity, thus ensuring a pseudo-ductile shear behavior, as explained previously.

Summary of Capacity Equations

This section is intended to give a summary of all the equations developed in this paper and to briefly highlight advantages and shortcomings of each of them. In Table 4 the capacity equations for $n = 1, 2$ are shown.

As discussed in the previous sections, the analytical method allows for the contribution of concrete in terms of strength to be accounted in the shear capacity; the application of this method requires the solution of the statically indeterminate structural model of Fig. 2. This has been done in this paper for the cases $n = 1$ and 2, giving Eqs. (31) and (32), respectively, reported in the first row of Table 4 as well. If one wants to evaluate the shear capacity for $n > 3$, provided that any other shear resisting mechanism be active and allows the third or fourth pair of tensile bars to yield, the same procedure can be applied and new equations can be developed. This surely represents a possible further development of this paper to be applied to longer spans.

The simplified (code compliant) method does not take into account the contribution of concrete in terms of strength, but only in terms of stiffness, as explained when introducing Eq. (34). This method has the advantage of giving simple formulations, useful for practicing engineers, and, as shown in Table 4, makes the calculation of the shear capacity very straightforward as the number of yielded bars increases because the only term $n_s = n$ has to be replaced in the expression of κ to obtain different values of shear capacity. As shown in "Correlation Studies," and as expected,

Table 4. Summary of Capacity Equations

Method	Number of pairs of yielded bars	
	$n = 1$	$n = 2$
Analytical	$V_{y1} = f_y A_b \sin\alpha (f_{AD} + \bar{X}/f_{AD} + \frac{2}{3} f_{AC} \cos^2\theta)$	$V_{y2} = f_y A_b \sin\alpha [\Delta^{ISO}/\Delta^{RED} - \Delta^{ISO}(1\text{–}2s/L)^{-1} + 1]$
Simplified (code compliant)	$V = \kappa f_{yd} A_b \sin\alpha$ with: $\kappa = n_t - 2(1-\delta_p)/n_t - 2(1-\delta_p) = 1$	$V = \kappa f_{yd} A_b \sin\alpha$ with: $\kappa = n_t - 2(1-\delta_p)/n_t - 2(2-\delta_p) > 1$
Standard	$V = f_{yd} A_b \sin\alpha$	N/A

Note: N/A = not available.

Downloaded from ascelibrary.org by University of California, Berkeley on 07/19/18. Copyright ASCE. For personal use only; all rights reserved.

simpler methods and equations yield more conservative values of shear capacity.

Then the standard method is the one currently in use to design CTBs in shear: it roughly evaluates the shear capacity as that attained at the yielding of the first pair of tensile bar, completely ignoring the contribution of concrete. This approach, beyond underestimating the shear capacity, does not properly represent the mechanical behavior of composite truss beams.

Conclusions

Starting from a comparative study with the well-known shear resisting mechanisms of RC structures, a mechanical model for CTBs was developed and shear capacity equations were derived from it. The proposed mechanical model stems from the concept that the shear capacity can be expressed as function of the force causing n web steel bars to yield before the concrete strut crushes. Two different capacity equations were proposed: the first one deriving from an analytical method that explicitly accounts for the contribution of concrete to the shear capacity and the second one obtained from a simplified (code compliant) method of analysis, which does not consider the concrete strut as a resisting element, having the relevant advantage of being much simpler for practical use and giving a more accurate evaluation of the shear strength than the standard method (Superior Council of Public Works Guidelines 2009), so allowing the optimization of the shear design.

The capability of the proposed models to capture the real structural behavior and the accuracy of the capacity equations have been verified by comparing the results of the equations with those of both nonlinear analyses and experimental tests. It was shown that the results of both the equations derived from the analytical and simplified (code compliant) method and the nonlinear analyses significantly agree with the experimental results, thus demonstrating that the current standard method largely underestimates the actual shear capacity and that by using the proposed capacity equations, a higher shear capacity can be exploited as a consequence of a better understanding of the mechanical behavior of CTBs.

Moreover, the paper presents a general methodology to derive shear capacity equations for CTBs, which can be conveniently applied to any topology once any other resisting mechanism is verified to be active in the structural element under consideration.

Appendix. Specimens: Materials

Concrete (MPa)					Steel (MPa)				
f_{cm}	f_{ck}	f_{cd}	f_{ctm}	E_{cm}	f_{ym}	f_{yk}	f_{yd}	f_{tk}	E_s
49.2	41.2	27.5	4.6	35,440	385.2	334.5	318.6	475.3	213,000

Note: Mechanical characteristics have been derived from 24 compression tests and 11 splitting tests on concrete cubes and cylinders, respectively, and 20 tensile tests on steel bars; subscript m denotes mean value, k denotes characteristic value, d denotes design value.

References

Connor, J. J. (1976). *Analysis of structural member systems*, Ronald Press Company, New York.

Fenwick, R. C., and Paulay, T. (1968). "Mechanisms of shear resistance of concrete beams." *J. Struct. Div.*, 94(ST10), 2235–2350.

Kent, D. C., and Park, R. (1971). "Flexural members with confined concrete." *J. Struct. Div.*, 97(ST7), 1969–1990.

Nielsen, M. P. (1998). *Limit analysis and concrete plasticity*, 2nd Ed., CRC Press, Boca Raton, FL.

Nielsen, M. P., and Braestrup, N. W. (1975). "Plastic shear strength of reinforced concrete beams." *Technical Rep. No. 3*, Vol. 46, Bygningsstatiske Meddelelser, Denmark.

OpenSees [Computer software]. Berkeley, CA, Pacific Earthquake Engineering Research Center, Univ. of California.

Park, R., and Paulay, T. (1975). *Reinforced concrete structures*, Wiley, New York.

Quaranta, G., Petrone, F., Marano, G. C., Trentadue, F., and Monti, G. (2010). "Structural design of composite concrete-steel beams with spatial truss reinforcement elements." *Asian J. Civ. Eng.*, 12(2), 155–178.

Scott, B. D., Park, R., and Priestley, M. J. N. (1982). "Stress-strain behavior of concrete confined by overlapping hoops at low and high strain rates." *J. Am. Concr. Inst.*, 79(1), 13–27.

Superior Council of Public Works. (2009). "Linee guida per l'utilizzo di travi travi tralicciate in acciaio conglobate nel getto di calcestruzzo collaborante e procedure per il rilascio dell'autorizzazione all'impiego." Rome.

Trentadue, F., Quaranta, G., Marano, G. C., and Monti, G. (2011). "Simplified lateral-torsional buckling analysis in special truss-reinforced composite steel-concrete beams." *J. Struct. Eng.*, 10.1061/(ASCE)ST.1943-541X.0000390, 1419–1427.

Downloaded from ascelibrary.org by University of California, Berkeley on 07/19/18. Copyright ASCE. For personal use only; all rights reserved.